

MULTI-STREAM FASTER RCNN WITH ELA FOR IMAGE TAMPERING DETECTION

Robin Elizabeth Yancey, Norman Matloff, Paul Thompson

ABSTRACT

With technological advances leading to an increase in mechanisms for image tampering, fraud detection methods must continue to be upgraded to match their sophistication. One problem with current methods is that they require prior knowledge of the method of forgery in order to determine which features to extract from the image to localize the region of interest. When a machine learning algorithm is used to learn different types of tampering from a large set of various image types, with a large enough database we can easily classify which images are tampered (by training on the entire image feature map for each image) [28]. However, we still are left with the question of which features to train on, and how to localize the manipulation. To solve this, object detection networks such as Faster R-CNN [22], which combine an RPN (Region Proposal Network) with a CNN, have recently been adapted to fraud detection by utilizing their ability to propose bounding boxes for objects of interest to localize the tampering artifacts [29]. By making use of the computational powers of today's GPUs this method also achieves a fast run-time and higher accuracy than the top current methods such as noise analysis, ELA (Error Level Analysis), or CFA (Color Filter Array) [29]. In this work, a multi-linear Faster RCNN network will be applied similarly but with the second stream having an input of the ELA JPEG compression level mask. This is shown to provide even higher accuracy by adding training features from the segmented image map to the network.

1. INTRODUCTION

Images are often trusted as evidence or proof in fields such as journalism, forensic investigations, military intelligence, scientific research and publications, crime detection and legal proceedings, investigation of insurance claims, and medical imaging [21]. In order to protect legal and political photos while maintaining research integrity or reproducibility, image manipulation detection is a highly necessary tool [7]. As technology advances, common image tampering techniques such as *retouching* or *resampling* which involves geometric

transformations on part of the image, *image splicing* which involves pasting a part of one image to another image, *copy-move* fraud which involves copying one part of the same image to another location within the photo [14], or *removal* which is the elimination of a region of the image by inpainting [29], are widely available to the public. Worse yet, this often includes post-processing such as Gaussian smoothing, making it even more difficult for humans to recognize the tampered regions with the naked eye. Due to the difficulty of distinguishing fake and authentic images, research in this field has become integral to preventing hacking.

A few of the most common and effective detection methods currently being used include the color filter array (CFA) [3], image noise analysis using noise filters [18], Discrete Cosine Transform (DCT) frequency analysis [11], Discrete Wavelet Transform (DWT), JPEG compression measurement using methods such as Block Artifact Grid (BAG) [27], and ELA (Error Level Analysis) [12], and many modifications of these [1] [6] [16] [28]. Detection of different methods such as copy-paste fraud, added WGN (White Gaussian Noise), and color enhancements, each require different filters and algorithms (eg. PCA, DWT, or DCT-based) which must also be applied at different sized bounding boxes depending on the size of the tampered region [11]. Additionally, the method needed often depends on the image type, such as JPEG, PNG, or TIFF [27]. This makes it difficult to determine which technique to apply to which image, since these details are often not provided. A method of detection that is generalizable to various differences between images or even new types of tampering is of great need today.

1.1. CNN for Tampering Detection

With the increase in image data available, and the increase in efficiency of modern GPUs to handle bigger problems, there has been interest in the application of machine learning for image fraud detection. These more sophisticated techniques have been able to train a model to estimate the probability of the images feature map (or sub-image feature blocks) being tampered [15]. Convolutional Neural Networks (CNN), are well suited for image tampering detection, and have been shown capable of detecting textures, noise, and resampling efficiently [2] [4] [5] [13] [25].

With the increase in use of deep-learning for these highly diverse image tasks, it was then found that networks which

This work was supported by Grant ORI2016000141 from the US Dept. of Health and Human Services. The ideas and implementation in this work are primarily the produce of the first author (RY). NM improved the presentation, while PT was the initiator of the overall image fraud project

are trained in object-detection can be adapted to manipulation detection [29]. Instead of proposing bounding boxes for objects of interest to localize the objects in the image, they localize the tampering artifacts by training on the manipulated dataset [29].

1.2. R-CNN

Specifically, Regional CNN (R-CNN) does the following: During training, a set of candidate regions of interest (RoIs) is generated, each possibly containing tampering, and then checked against ground truth, is as follows:

```
image data ->
generate RoIs ->
CNN layers ->
dense layers ->
tampering classification
```

Various refinements exist that make the generation and checking of the numerous RoIs more efficient. These include Fast R-CNN and Faster R-CNN.

Subsequent work [29] improved the accuracy of image forgery detection over previous methods by using a bilinear approach. By simultaneously examining both the RGB image content and noise information [19], a combination of techniques is employed for tampering detection:

```
image data ->
RPN: generate candidate RoIs ->
conv. layers ->
stream1=RGB, stream2=Noise ->
dense layers ->
tampering classification
```

- stream 1, the RGB channels, are able to capture inconsistencies at tampered boundaries.
- stream 2, models local Noise, which may vary between the target image and the spliced portion

The output of the CNN is fed both into the stream1 and stream2 filters, both of which become features, which are combined in an outer product operation [17].

1.3. The Present Work

Here we use ELA instead of Noise:

```
image data ->
RPN: generate candidate RoIs ->
CNN layers RoIs ->
stream1=RGB, stream2=ELA ->
dense layers ->
tampering classification
```

The ELA stream is essential. Each 8×8 block in an image will have a Quality level. The various blocks of a given image will typically have similar levels. But when part of the source image is removed and pasted into the target image, the pasted section will likely have a Quality level substantially different from the other parts of the picture.

Our preliminary work showed that ELA performs the best image segmentation compared to other current methods listed above and works just as well on non-JPEG images since the compression levels will still be different. Thus it makes sense to use this as stream2.

2. METHODS

The framework presented here builds on the Faster RCNN network [22], with two streams instead of one. The RGB stream takes an input of all three color channels from the image, making it most efficient for measuring color and lighting changes. The JPEG compression stream will have an input of the Error Level Analysis (ELA) [12] of the image to provide additional evidence of manipulation. This technique is a modification to the bilinear Faster RCNN in [29], which used a noise filter as the second stream input; we use ELA instead.

2.1. JPEG Compression Analysis Stream

The Error Level Analysis (ELA) output is a greyscale heatmap image that is created as follows: One saves the image at a slightly lower JPEG Quality level, reads it back in, and computes the pixel-by-pixel difference within 8×8 blocks from the original image. Since image regions with lower Quality in the original image will degrade at a higher rate when compressed, subtracting the decompressed image from the original image gives the difference in Quality levels in each block. Image blocks that originally had lower Quality levels will have the highest error and brightest color in the greyscale output heatmap since the pixel values are higher. The steps of ELA are summarized below:

- read in image as JPEG
- write image as JPEG with Quality lower level (eg. 90)
- read in compressed image (decompress)
- take absolute value of the difference between the decompressed image in step 3 and the original image in step 1

Since the RGB stream alone has been shown to be highly accurate in detection of manipulated regions [29], only this stream provides the region proposals of the RPN layer. Before being combined with the JPEG compression layer for RoI (Regions of Interest) pooling, the RoIs produced by the RPN of the RGB stream are used for bounding box regression to provide a localized box around the region including

detection accuracy measures. After the two streams are fused through multi-stream pooling, they are input into the fully connected layer for manipulation classification [29].

The loss for the RPN network is defined as

$$L_{RPN}(g_i, f_i) = \frac{1}{N_{cls}} \sum_i L_{cls}(g_i, g_i^*) + \lambda \frac{1}{N_{reg}} \sum_i g_i^* L_{reg}(f_i, f_i^*)$$

- g_i represents the probability of anchor i being a manipulated region in a mini batch,
- g_i^* is the ground-truth label for anchor i to be manipulated
- f_i, f_i^* are the four dimensional bounding box coordinates for anchor i and the ground-truth, respectively
- L_{cls} denotes cross entropy loss for RPN network and L_{reg} denotes smooth L_1 loss for regression
- N_{cls} denotes the size of a mini-batch
- λ is a hyper-parameter to balance the two losses

2.2. Multi-Stream Pooling

Multi-stream pooling is used to combine both streams while maintaining the spatial information between each of the pixels in the images being processed through each stream [29]. The output of the multi-stream pooling layer is $x = f_{RGB}^T f_{JPGC}$, where f_{RGB} is the RoI of the RGB stream and f_{JPGC} is the RoI of the JPEG compression analysis stream. The predicted classes of the Regions of Interest are output from the network's fully connected and soft-max layers and cross entropy loss is used for classification and smooth L_1 loss for bounding box regression [29]. The total loss function is the sum of all of the features as shown below:

$$L_{total} = L_{RPN} + L_{tamper}(f_{RGB}, f_{JPGC}) + L_{bbox}(f_{RGB})$$

where

- L_{total} denotes total loss
- L_{RPN} denotes the RPN loss
- L_{tamper} denotes the final cross entropy classification loss (based on the output of multi-stream pooling)
- L_{bbox} denotes the final bounding box regression loss
- f_{RGB} represents the RoI from the RGB stream
- f_{JPGC} represents the RoI from the JPEG compression stream

2.3. Implementation

The model was implemented in Python with a slightly modified version of the Faster RCNN library [23] on a Quadro 6000 GPU. The network was first trained and tested on a pre-generated spliced image database constructed from the PASCAL VOC data [9], by digitally selecting the random objects by their bounding boxes provided in each dataset, and pasting them into another image, moving the new object bounding box annotation with it. Second, it was trained and tested on subsets of a few traditional image manipulation datasets.

3. RESULTS

3.1. Synthetic Dataset Tests

The spliced image in Figure 1, from the CASIA [8], database, will be used to show an example of the output of ELA and the Faster-RCNN network model. The cat in the image has been cut out and pasted from another image.



Fig. 1. Example Tampered Input Image

The output of the ELA filter applied to the cat image is shown in Figure 2.

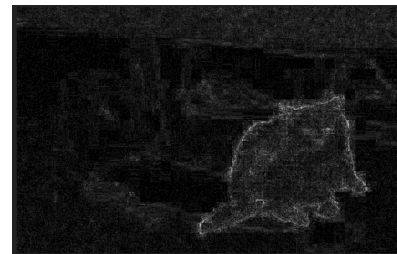


Fig. 2. Output of Error Level Analysis Localization

Figure 3 shows the output Faster R-CNN with the RGB stream only model applied to the cat image.



Fig. 3. Output of the Faster-RCNN Model

The output from the multi-stream model (with ELA) is shown on in the figure below (having slightly higher accuracy).



Fig. 4. Output of the Multi-Stream Faster-RCNN Model with ELA

The model was tested using the test function provided in Faster RCNN library [23] based on the evaluation metric for PASCAL VOC project [10]. The AP score that this metric computes is based on the precision and recall. The precision measures how accurate the predictions are using the percentage of the correct predictions out of the total (where FP represents the number of false positive predictions and TP is the number of true positive predictions), as shown below:

$$Precision = \frac{TP}{FP + TP} \quad (1)$$

The recall measures how well all the positives are found in the test set (where FN is the number of false negative guesses), as shown below

$$Recall = \frac{TP}{FN + TP} \quad (2)$$

The Intersection over Union (IoU) is the overlap between the predicted bounding box coordinates and those from the ground truth image. For the PASCAL VOC project, the prediction is positive if the IoU is greater than 0.5. Average Precision (AP) is calculated based on an average of the 11-point recall values. Specifically, the AP is calculated as shown below,

$$AP = \frac{1}{11} \sum_{r \in \{0.0, \dots, 1.0\}} AP_r \quad (3)$$

$$= \frac{1}{11} \sum_{r \in \{0.0, \dots, 1.0\}} P_{interp}(r) \quad (4)$$

where $P_{interp}(r)$ is the precision at the recall value r .

When both the test set and the training set consisted of 5k synthetic PASCAL VOC images, the AP score was .90 (averaged over 3 tests on different test sets generated separate from the training set). Figure 5 shows two examples of the visualizations of the predicted boxes on the PASCAL VOC synthetic training set. The top images show the original untampered images from the dataset while the bottom ones show the manipulated images with bounding box coordinates around the predicted region.



Fig. 5. Tests on the PASCAL VOC [9] Synthetic Dataset, Top: Untampered Image, Bottom: Synthetic Tampered Image with Predictions

3.2. Official Image Manipulation Dataset Tests

Secondly, the network was trained on a few official image manipulation datasets such as subsets of CASIA 1 & 2 [8], CoMoFoD [24], and COVER [26]. Only those images from CASIA 1 & 2 with clear bounding boxes were used for testing so that it would be easy to make a fair judgement of the overall prediction accuracy on this dataset. The test sets were randomly selected from the full set of images before training. Since, training beyond 45k steps did not improve accuracy, each training session was stopped prior to this point and lower numbers of were used forsteps for those datasets with less images. The PNG images from CoMoFoD and the TIFF images from CASIA were converted to JPEG before being input into the ELA function. Table 1 summarizes the results of these tests compared to synthetic.

Figure 6 shows additional examples of visualizations of results from tests on images from the CoMoFoD and Image Manipulation Datasets [6]. Clearly, each prediction with the ELA stream is better than the single model alone, because the second stream helps to remove false positives by providing additional training features based on the level of compression of the manipulated regions compared to that of the original image.

Dataset	Test/Train	Train Steps	AP
Synthetic	5k/5k	45k	0.90
COVER	10/100	15k	0.82
CASIA	50/2886	25k	0.69
CoMoFoD	15/143	20k	0.59

Table 1. Tests on Manipulated Datasets

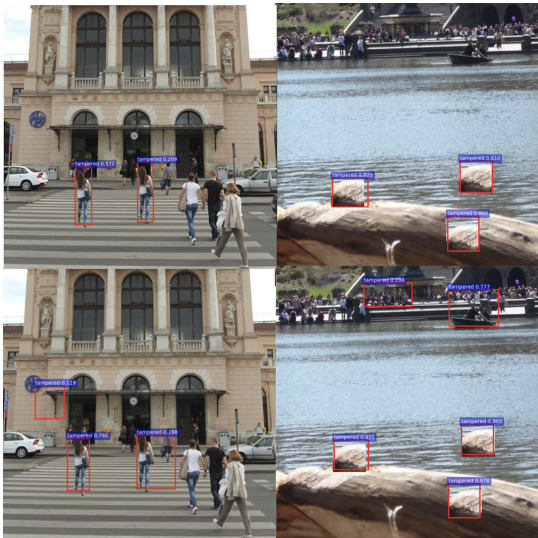


Fig. 6. Top: Output of the Multi-Stream Faster-RCNN Model with ELA on PNG Images, Bottom: Output of the Faster-RCNN Model

4. DISCUSSION

Both the Faster R-CNN model and the multi-stream version were able to effectively localize tampered regions from the traditional image databases [8], which shows that this proposed model is useful for detecting image fraud. The predicted accuracy of the tampered region, the proposed coordinates of the bounding box, and the FP rate are more accurate in the multi-stream model with ELA. Further, although the test set is different, the AP is higher than those in Table 1 in their paper in [29] and would likely be similar to results in table 7 if tested on NIST16 (since AUC seems to be close to AP). Based on a comparison of the output images and the results from [29] it is likely to be robust to BAG, ELA, noise analysis, DCT, and RLRN detection [20] on any image while having much clearer and more precise results. This implementation is also highly generalizable since non-JPEG images can be converted to JPEG prior to being input to the model for ELA without loss of prediction accuracy. These previous methods

also lack a feature to place a bounding box with its accuracy over the localized region. Older methods normally use a sliding window of feature maps derived from fixed size box of image pixels to test for manipulated regions, while this network uses bounding box regression on various anchor box sizes to estimate the probability of a region being tampered allowing us to simultaneously capture more information within regions of the image. The ability to predict the RoI helps produce far less false positives by making the location of the region less ambiguous than previous methods. Future work involves training on the synthetic dataset prior to fine-tuning the network with the multiple combined traditional image manipulation databases, as well as testing a model with 3 or more streams. These tests will also be evaluated with similar metrics (F1 and AUC) to be directly compared to [29].

5. REFERENCES

- [1] C. N. Bharti and P. Tandel. A survey of image forgery detection techniques. In *2016 International Conference on Wireless Communications, Signal Processing and Networking (WiSPNET)*, pages 877–881, March 2016.
- [2] L. Bondi, S. Lameri, D. Gera, P. Bestagini, E. J. Delp, and S. Tubaro. Tampering detection and localization through clustering of camera-based cnn features. In *2017 IEEE Conference on Computer Vision and Pattern Recognition Workshops (CVPRW)*, pages 1855–1864, July 2017.
- [3] H. Cao and A. C. Kot. Accurate detection of demosaicing regularity for digital image forensics. *IEEE Transactions on Information Forensics and Security*, 4(4):899–910, Dec 2009.
- [4] J. Chen, X. Kang, Y. Liu, and Z. J. Wang. Median filtering forensics based on convolutional neural networks. *IEEE Signal Processing Letters*, 22(11):1849–1853, Nov 2015.
- [5] H. Choi, H. Jang, D. Kim, J. Son, S. Mun, S. Choi, and H. Lee. Detecting composite image manipulation based on deep neural networks. In *2017 International Conference on Systems, Signals and Image Processing (IWSSIP)*, pages 1–5, May 2017.
- [6] V. Christlein, C. Riess, J. Jordan, C. Riess, and E. Angelopoulos. An evaluation of popular copy-move forgery detection approaches. *IEEE Transactions on Information Forensics and Security*, 7(6):1841–1854, Dec 2012.
- [7] Douglas W. Crome. Avoiding twisted pixels: Ethical guidelines for the appropriate use and manipulation of scientific digital images. *Science and engineering ethics*, 16 4:639–67, 2010.

- [8] J. Dong, W. Wang, and T. Tan. Casia image tampering detection evaluation database. In *2013 IEEE China Summit and International Conference on Signal and Information Processing*, pages 422–426, July 2013.
- [9] M. Everingham, L. Van Gool, C. K. I. Williams, J. Winn, and A. Zisserman. The PASCAL Visual Object Classes Challenge 2012 (VOC2012) Results. <http://www.pascal-network.org/challenges/VOC/voc2012/workshop/index.html>.
- [10] M. Everingham, L. Van Gool, C. K. I. Williams, J. Winn, and A. Zisserman. The pascal visual object classes (voc) challenge. *International Journal of Computer Vision*, 88(2):303–338, June 2010.
- [11] Jessica Fridrich, David Soukal, and Jan Luks. Detection of copy-move forgery in digital images. *Int. J. Comput. Sci. Issues*, 3:55–61, 01 2003.
- [12] Teddy Surya Gunawan, Siti Amalina Mohammad Hanafiah, Mira Kartiwi, Nanang Ismail, Nor Farahidah Zabab, and Anis Nurashikin Nordin. Development of photo forensics algorithm by detecting photoshop manipulation using error level analysis. In *CVPR*, 2017.
- [13] N. Huang, J. He, and N. Zhu. A novel method for detecting image forgery based on convolutional neural network. In *2018 17th IEEE International Conference On Trust, Security And Privacy In Computing And Communications/ 12th IEEE International Conference On Big Data Science And Engineering (TrustCom/BigDataSE)*, pages 1702–1705, Aug 2018.
- [14] Abhishek Kashyap, Rajesh Singh Parmar, M Agarwal, and Hari Gupta. An evaluation of digital image forgery detection approaches. *International Journal of Applied Engineering Research*, 12:4747–4758, 03 2017.
- [15] K. Khuspe and V. Mane. Robust image forgery localization and recognition in copy-move using bag of features and svm. In *2015 International Conference on Communication, Information Computing Technology (ICCICT)*, pages 1–5, Jan 2015.
- [16] Hwei-Jen Lin, Chun-Wei Wang, and Yang-Ta Kao. Fast copy-move forgery detection. *WSEAS Trans. Sig. Proc.*, 5(5):188–197, May 2009.
- [17] Tsung-Yu Lin, Aruni Roy Chowdhury, and Subhransu Maji. Bilinear cnn models for fine-grained visual recognition. In *Proceedings of the 2015 IEEE International Conference on Computer Vision (ICCV), ICCV '15*, pages 1449–1457, Washington, DC, USA, 2015. IEEE Computer Society.
- [18] Bo Liu, Chi-Man Pun, and Xiaochen Yuan. Digital image forgery detection using jpeg features and local noise discrepancies. *TheScientificWorldJournal*, 2014:230425, 03 2014.
- [19] Babak Mahdian and Stanislav Saic. Using noise inconsistencies for blind image forensics. *Image Vision Comput.*, 27(10):1497–1503, September 2009.
- [20] A. H. Mir, M. Hanmandlu, and S. N. Tandon. Texture analysis of ct images. *IEEE Engineering in Medicine and Biology Magazine*, 14(6):781–786, Nov 1995.
- [21] Minati Mishra and Munesh Adhikary. Digital image tamper detection techniques - a comprehensive study. 06 2013.
- [22] S. Ren, K. He, R. Girshick, and J. Sun. Faster r-cnn: Towards real-time object detection with region proposal networks. *IEEE Transactions on Pattern Analysis and Machine Intelligence*, 39(6):1137–1149, June 2017.
- [23] Shaoqing Ren, Kaiming He, Ross Girshick, and Jian Sun. Faster R-CNN: Towards real-time object detection with region proposal networks. In *Advances in Neural Information Processing Systems (NIPS)*, 2015.
- [24] Dijana Tralic, Ivan Zupancic, Sonja Grgic, and Mislav Grgic. Comofod -new database for copy-move forgery detection. 09 2013.
- [25] Y. Wei, X. Bi, and B. Xiao. C2r net: The coarse to refined network for image forgery detection. In *2018 17th IEEE International Conference On Trust, Security And Privacy In Computing And Communications/ 12th IEEE International Conference On Big Data Science And Engineering (TrustCom/BigDataSE)*, pages 1656–1659, Aug 2018.
- [26] Bihan Wen, Ye Zhu, Ramanathan Subramanian, Tian-Tsong Ng, Xuanjing Shen, and Stefan Winkler. Coverage a novel database for copy-move forgery detection. In *IEEE International Conference on Image processing (ICIP)*, pages 161–165, 2016.
- [27] S. Ye, Q. Sun, and E. Chang. Detecting digital image forgeries by measuring inconsistencies of blocking artifact. In *2007 IEEE International Conference on Multimedia and Expo*, pages 12–15, July 2007.
- [28] Xudong Zhao, Jianhua Li, Shenghong Li, and Shilin Wang. Detecting digital image splicing in chroma spaces. In Hyoung-Joong Kim, Yun Qing Shi, and Mauro Barni, editors, *Digital Watermarking*, pages 12–22, Berlin, Heidelberg, 2011. Springer Berlin Heidelberg.
- [29] Peng Zhou, Xintong Han, Vlad I. Morariu, and Larry S. Davis. Learning rich features for image manipulation detection. In *CVPR*, 2018.